

Electronic Supplementary Information

**A supramolecular hydrogel with monitorable macro-
/microscopic shape memory performance**

Wu Wang,^{‡a} Hua Lai,^{‡a} Zhongjun Cheng,^b Zhimin Fan,^a Haiyang Zhang,^a Jingfeng
Wang,^a Songji Yu,^a and Yuyan Liu^{*a}

^aMIT Key Laboratory of Critical Materials Technology for New Energy Conversion
and Storage, School of Chemistry and Chemical Engineering, Harbin Institute of
Technology, Harbin 150001, China

^bAcademy of Fundamental and Interdisciplinary Sciences, Harbin Institute of
Technology, Harbin, Heilongjiang 150090, China.

*Corresponding authors Email: liuyy@hit.edu.cn, Fax: +86 045186402368

‡These authors contributed equally

Experimental

1. Materials

Phenylboronic acid (PBA), N,N'-Methylenebisacrylamide (MBA), Ammonium persulfate (APS), Acrylamide (AAm), and Polyvinyl alcohol (PVA) with an alcoholysis degree of 99% (the average degree of polymerization is about 1700) were supplied by Aladdin Chemical Co., Ltd. HCl (36.0–38.0%) and NaOH (AR) were purchased from Sinopharm Chemical Reagent Co., Ltd. Polytetrafluoroethylene (PTFE) membranes (the average pore size is about 0.22 μm) were provided by Sartorius. Dialysis bag (molecular weight cutoff 1000 Da) was purchased from Viskase. All aqueous solutions were prepared using ultrapure water with a resistivity of 18.2 $\text{M}\Omega\text{ cm}^{-1}$.

2. Synthesis of the fluorescent CQDs

The CQDs were prepared through a facile hydrothermal method as reported.¹ Firstly, 0.6 g PBA and 60 mL ultrapure water were placed into a 100 mL hydrothermal reactor, and the pH value of solution was adjusted to 12 by adding NaOH; then, the solution was heated at 220 $^{\circ}\text{C}$ for 12 h. After cooling to room temperature, the prepared solution was filtered with a 0.22 μm PTFE membrane. To further purify the CQDs, the resultant solution was dialyzed in a dialysis bag for 48 h. Finally, the purified CQDs were freeze-dried to obtain solid CQDs for further use.

3. Synthesis of supermolecular SMHs

First, PVA was dissolved in pure water at 90 $^{\circ}\text{C}$ for 2 h; meanwhile, a certain amount of CQDs were added in the solution and gradually mixed and stirred at 90 $^{\circ}\text{C}$ for another

3 h, After that, the obtained mixture was poured into a beaker and cooled to room temperature. Then, the AAm, MBA and APS were added into the mixture under ultrasonic treatment for 30 min to obtain the homogeneous solution. Finally, the mixture was poured into a mold and further kept in a water bath kettle at 60 °C for 8 h to prepare SMHs. To investigate the influence of the crosslinking density on the shape memory property of the SMHs better, we designed four samples respectively. The specific composition of all SMHs samples is shown in Table S1.

4. Shape memory performance of supermolecular SMHs

Shape memory performance of the hydrogel in macroscale was measured by a bending test. Firstly, a straight strip of hydrogel (30 mm × 4 mm × 1 mm) was bent to an angle (θ_o) of about 180°. Then, the bent strip was further put in to base solution (pH=12) under external force, and then, the deformed shape (θ_i) was obtained. Subsequently, the shape recovery performance was investigated by immersing the deformed strip into acid water (pH=2) to record the change of bending angle (θ_f) with the increase of immersion time. The shape fixity ratio (R_f) and the shape recovery ratio (R_r) in macroscale were defined as the following equations (1) and (2) :

$$R_f = \frac{\theta_i}{\theta_o} \quad (1)$$

$$R_r = \frac{\theta_i - \theta_f}{\theta_i} \quad (2)$$

Shape memory performance of the hydrogel in microscale was measured through laser scanning confocal microscopy. Firstly, a thin layer of the as-synthesized hydrogel

was deposited on a glass substrate. Then, a structured epoxy resin stamp (the average height was marked as H_o) was applied in contact with the hydrogel surface with a gentle force to create micropatterns through microcontact printing. After treated in the alkaline solution following the removal of the stamp, the average fixed depth (H_f) of the hydrogel was obtained. Subsequently, the shape recovery performance was investigated by immersing the deformed hydrogel into acid water (pH=2) to record the change of average depth (H_r) with the increase of immersion time. The shape fixity ratio (R_f) and the shape recovery ratio (R_r) in microscale were defined as the following equations (2) and (4) :

$$R_f = \frac{H_f}{H_o} \quad (3)$$

$$R_r = \frac{H_f - H_r}{H_f} \quad (4)$$

5. Instruments

Transmission electron microscopy (TEM) and high-resolution TEM (HRTEM) images were obtained with a transmission electron microscope (Tecnai G2 F30, USA) at an accelerating voltage of 300 kV. Atomic force microscopy (AFM) was performed using a commercial Bruker Multimode 8 AFM system in contact mode (Bruker, USA).

Scanning electron microscopy (SEM) image was obtained a scanning electron microscope (Carl Zeiss, Germany). The microscale morphology and corresponding profile curves were recorded on a laser scanning confocal microscope (Olympus,

Japan). X-ray photo electron spectroscopy (XPS) analysis was done with Al, K as the excitation source on a Thermo Fisher Scientific K-Alpha 1063 X-ray photoelectron spectrometer (Britain). Fourier transform infrared spectra (FT-IR) in the 4000 to 400 cm^{-1} regions were recorded on a Nicolet Nexus 670 FT-IR spectroscope (Nicolet Instrument Co., USA). Fluorescence spectra were measured on a fluorescence spectrophotometer (PerkinElmer, UK). The UV-Vis spectra were obtained from a UV-2450 UV-Vis spectrophotometer (Shimadzu Co., Japan)

Table S1. Specific formula of SMH

Sample	CQDs [g]	PVA [g]	AAM [g]	MBA [mg]	APS [mg]	Water content [%]
S1	0.05	0.5	1.8	0.6	18	82
S2	0.05	0.5	1.8	1.2	18	82
S3	0.05	0.5	1.8	2.0	18	82
S4	0.05	0.5	1.8	3.0	18	82

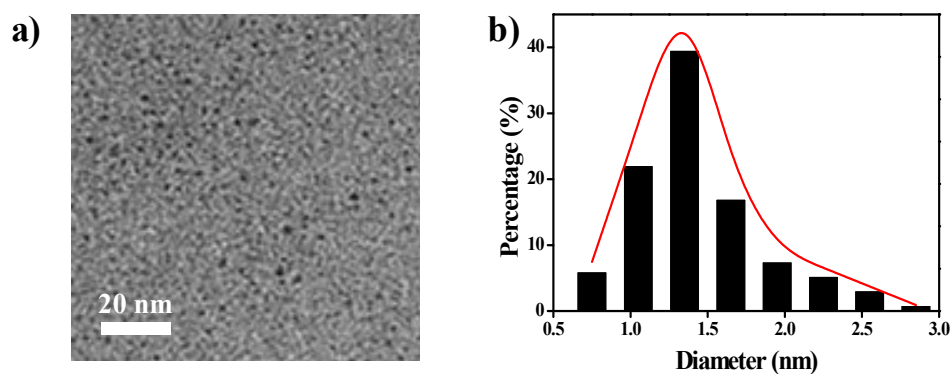


Fig.S1 (a) TEM image of CQDs. (b) Size distribution of CQDs.

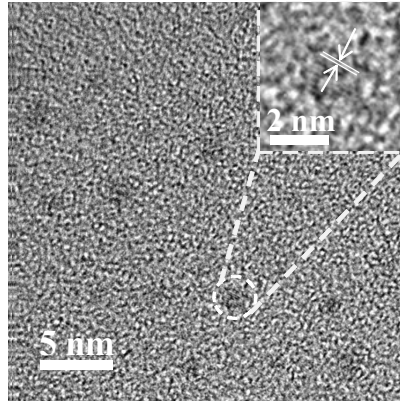


Fig. S2 HRTEM image of CQDs with lattice parameters of 0.21 nm.

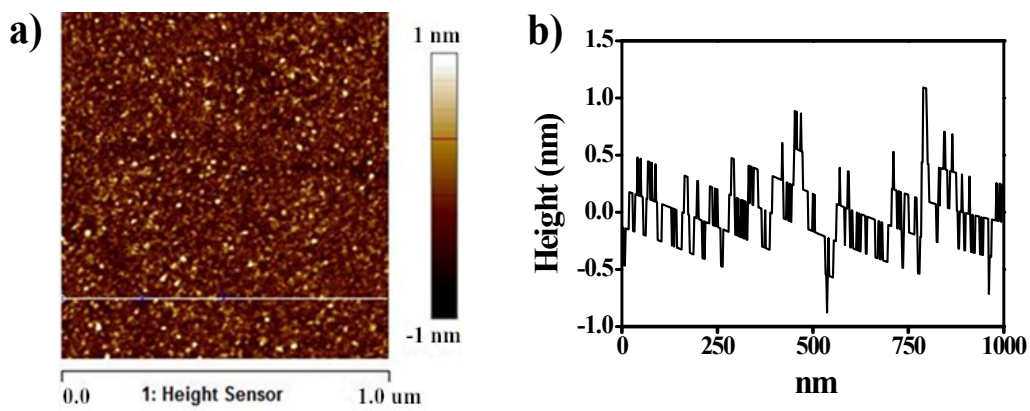


Fig. S3 (a) AFM image of CQDs. (b) Height profile of CQDs

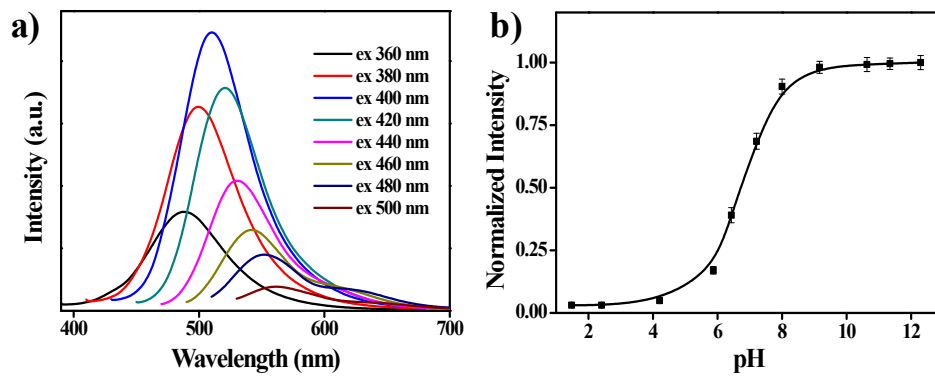


Fig.S4 (a) Fluorescence spectra of CQDs at different excitation wavelengths ranging from 360 nm to 500 nm. (b) Fluorescence intensity of CQDs at different pH values.

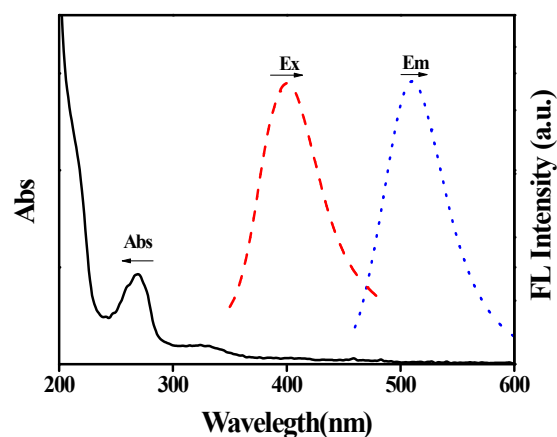


Fig. S5 UV/Vis and fluorescence excitation and emission spectra of the CQDs.

As shown in Fig. S5, the absorption peak in the region at about 270 nm in the UV/Vis spectrum of CQDs is ascribed to the $\pi-\pi^*$ transition of the aromatic sp^2 domains of the C=C bond. The shoulder peak at about 330 nm is ascribed to the $n-\pi^*$ transition of the C=O bond. The as-prepared CQDs show the maximum excitation wavelength and maximum emission wavelength at 400 nm and 510 nm, respectively.

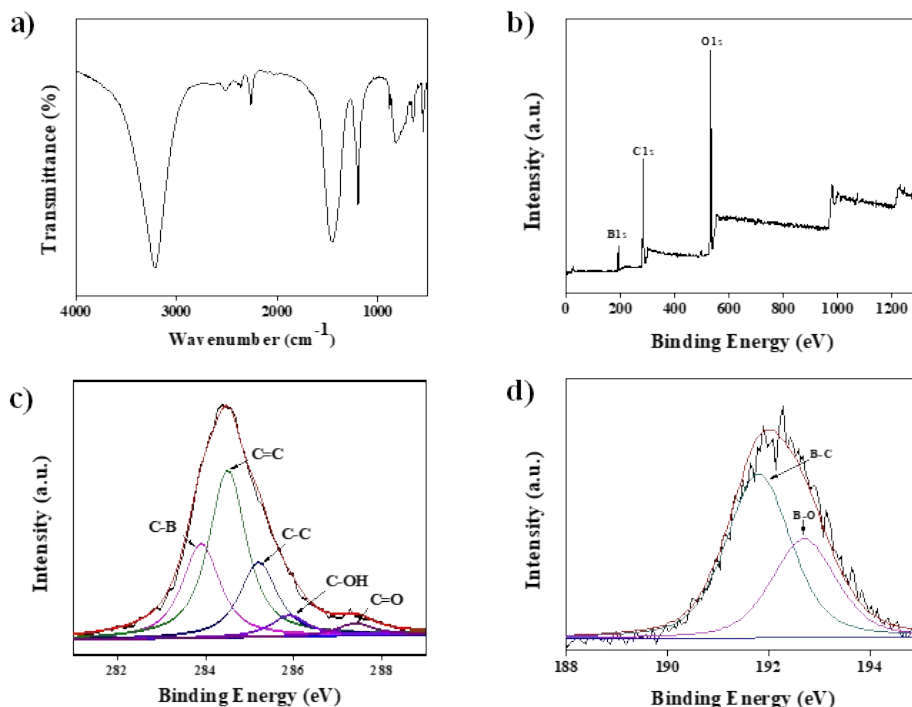


Fig. S6 (a) FT-IR spectra of CQDs. (b) XPS survey spectra of CQDs. (c) C 1s XPS spectra of CQDs and (d) B 1s XPS spectra of CQDs.

The chemical properties of the prepared CQDs were further examined by the FT-IR and XPS analysis. As shown in Fig. 6a, in the FT-IR spectra, the strong absorption band at about 1195 cm^{-1} corresponds to the bending vibration of B–O–H.² The bands at about 878 cm^{-1} and 647 cm^{-1} can be assigned to the out-of-plane deformation vibration of the aromatic C–H. The weak shoulder peaks at about 1343 cm^{-1} and 1090 cm^{-1} can be ascribed to the stretching vibration of B–O and C–B,³ respectively. Fig. 6b is the XPS survey spectra of the as-prepared CQDs. The three peaks at about 284.4 eV of C 1s, 532.4 eV of O 1s and 192.1 eV of B 1s, can be observed respectively. As shown in Fig. 6c, from the high-resolution carbon spectra, the C 1s spectrum can be decomposed into five peaks corresponding to the following functional groups: C–B at 283.9 eV , C=C at 284.5 eV , C–C at 285.2 eV , C–OH at 285.9 eV and C=O at 287.4 eV ,⁴ respectively. Similarly, as shown in Fig. 3d, the B 1s can be decomposed into two peaks of B–C at 191.8 eV and B–O at 192.7 eV , respectively.¹ These results indicate that the surface of the as-synthesized CQDs were covered by various functional groups including –COOH, –OH, and –B(OH)₂.

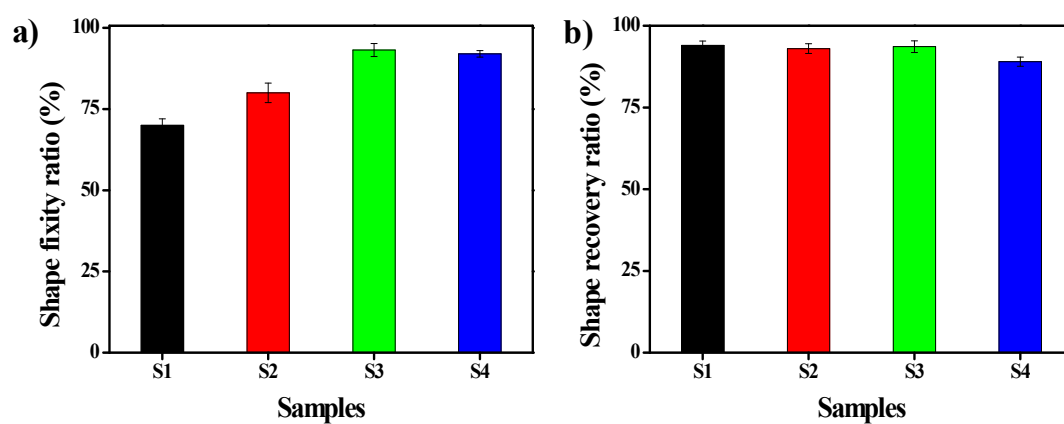


Fig. S7 (a) shape fixity ratio of all samples in base water (pH=12). (b) shape recovery ratio of all samples in acid water (pH=2).

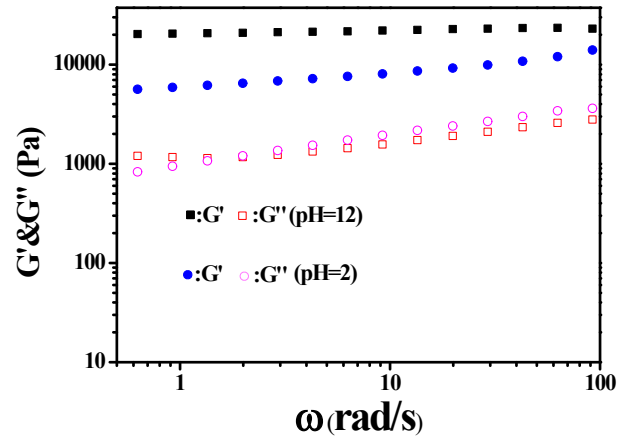


Fig. S8 Storage modulus (G') and loss modulus (G'') of hydrogel treated in alkaline (pH=12) and acid (pH=2) condition, respectively.

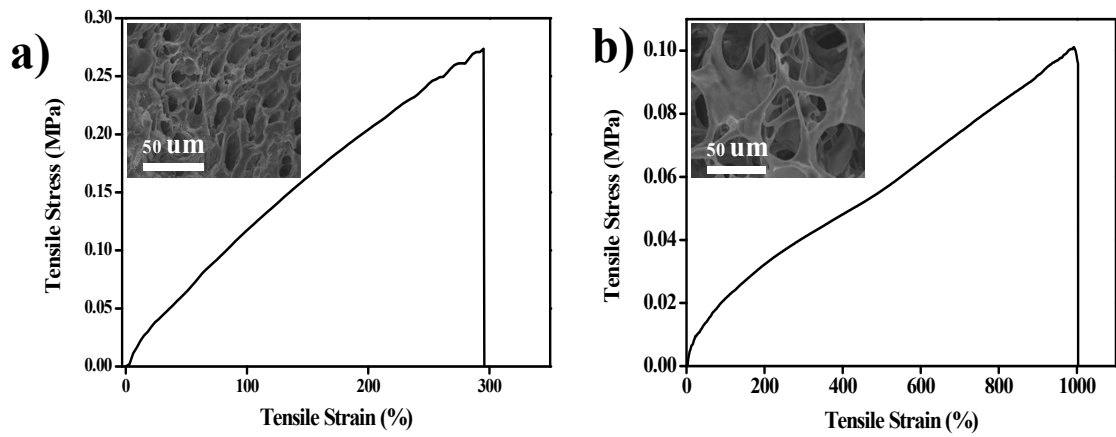


Fig. S9 (a) Tensile stress-strain curves of S3 treated in alkaline condition (pH=12). (b) Tensile stress-strain curves of S3 treated in acid condition (pH=2). Inset are corresponding SEM image.

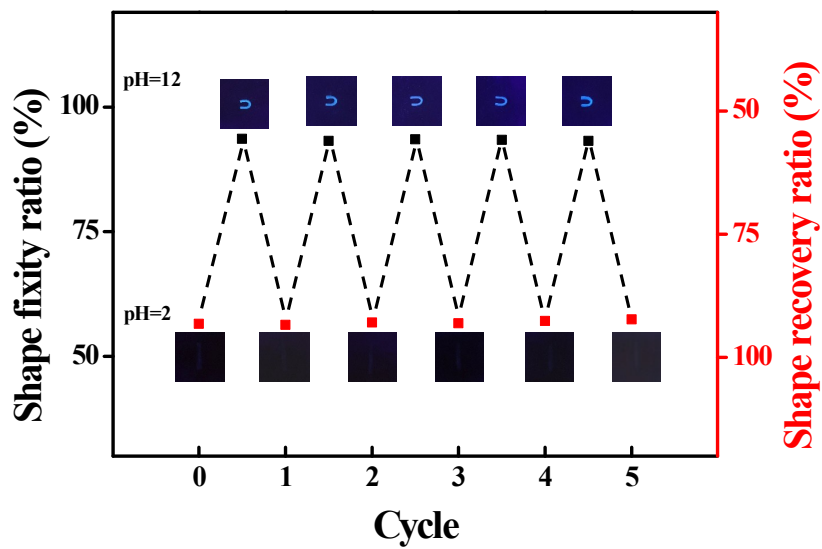


Fig. S10 Shape memory cycle of SMH.

References

- 1 W. Wang, H. Lai, Z. Cheng, H. Kang, Y. Wang, H. Zhang, J. Wang and Y. Liu, *J. Mater. Chem. B*, **2018**, 6, 7444-7450.
- 2 P. Shen, Y. Xia, *Anal. Chem.*, 2014, **86**, 5323-5329.
- 3 S.H. Brewer, A.M. Allen, S.E. Lappi, T.L. Chasse, K.A. Briggman, C.B. Gorman, S. Franzen, *Langmuir*, 2004, **20**, 5512-5520.
- 4 Q. Lu, C. Wu, D. Liu, H. Wang, W. Su, H. Li, Y. Zhang, S. Yao, *Green. Chem.*, 2017, **19**, 900-904.